Green synthesis of FeO nanoparticles from coffee and its application for antibacterial, antifungal, and anti-oxidation activity

ALANGARI, Abdulaziz, ALQAHTANI, Mohammed S., SHAHID, Mudassar, SYED, Rabbani, GOEL, Mukesh <http://orcid.org/0000-0003-2991-3439>, LAKSHMIPATHY, R. and KAUR, Kirtanjot

Research Article

Abdulaziz Alangari, Mohammed S. Alqahtani, Mudassar Shahid, Rabbani Syed*, Mukesh Goel, R. Lakshmipathy*, and Kirtanjot Kaur

Green synthesis of FeO nanoparticles from coffee and its application for antibacterial, antifungal, and anti-oxidation activity

https://doi.org/10.1515/gps-2023-0268
received December 26, 2023; accepted April 01, 2024

Abstract: This study presents a sustainable method for producing iron oxide nanoparticles (FeO NPs) using aqueous extracts from coffee seeds. Characterization through X-ray diffraction (XRD), scanning electron microscopy, and transmission electron microscopy (TEM) revealed non-spherical NPs ranging from 30 to 50 nm. The XRD analysis confirmed that the face-centred cubic structure and the Debye–Scherrer's crystalline size support the FeO particle size confirmed from TEM. The synthesized NPs demonstrated significant antimicrobial activity against *Escherichia coli* and *Staphylococcus aureus*, as well as antifungal activity against *Aspergillus niger*. Additionally, they exhibited potent antioxidant properties, effectively inhibiting DPPH, α-amylase, and α-glucosidase compared to acarbose and coffee extract. The findings suggest that these FeO NPs hold promise as antimicrobial, antioxidant, antifungal, and potentially antidiabetic agents.

Keywords: anti-microbial, anti-oxidation, coffee, iron oxide nanoparticles, green synthesis

*** Corresponding author: Rabbani Syed,** Department of Pharmaceutics, College of Pharmacy, King Saud University, Riyadh 11451, Saudi Arabia, e-mail: rsyed@ksu.edu.sa
*** Corresponding author: R. Lakshmipathy,** Directorate of Learning and Development, SRM Institute of Science and Technology, Kattankulathur, 603203 Tamil Nadu, India, e-mail: lakshmipathy.vit@gmail.com
Abdulaziz Alangari: Department of Clinical Laboratory Sciences, College of Applied Medical Sciences, King Saud University, Riyadh 11433, Saudi Arabia
Mohammed S. Alqahtani, Mudassar Shahid: Department of Pharmaceutics, College of Pharmacy, King Saud University, Riyadh 11451, Saudi Arabia
Mukesh Goel: Department of Engineering and Maths, College of Business, Technology and Engineering, Sheffield Hallam University, Sheffield, United Kingdom
Kirtanjot Kaur: Department of Chemistry, University Centre for Research and Development, Chandigarh University, Mohali, Punjab, India

1 Introduction

Nanotechnology is the ground-breaking technique that comprises managing molecules at the level of nanoscale. The field has become exciting for modern technology as it makes particles of different sizes, chemical properties, textures, dimensions, and shapes. All these products have different properties and applications. The properties of nanoparticles (NPs) differ from their bulk counterparts as a result of their size. Materials at the nanoscale have been extremely progressive in terms of knowledge and applications [1–3]. NPs fall into three main categories based on their composition: metallic, ceramic, and polymeric. Metallic NPs find applications in diverse fields like textiles, food, agriculture, health, and cosmetics. Their small size grants them a high surface area-to-volume ratio, significantly influencing their physical and chemical properties [4]. This alteration enhances their potential utility across various applications, owing to the improvements in their properties [5].

Iron oxide (FeO) NPs are the simplest and smallest particles of iron and they display high surface area and reactivity. These particles are not toxic in nature and display exceptional stability in terms of dimensions. FeO NPs have great electrical and thermal stabilities and have a good magnetic effect [6]. On oxidation of FeO by exposure to air and water, free ions of Fe are produced. FeO NPs can be used for various applications such as drug delivery, separation, dye adsorption, photocatalysis, imaging, etc. [7,8]. NPs of FeO have been recognized to play a major role as conducting materials. Due to these unique and attractive properties, a lot of research has been carried out on fabricating FeO NPs. Recently, methods such as sol–gel, chemical precipitation, flow injection, ultrasonic, electro-chemical, and hydrothermal have been developed for the synthesis of FeO NPs [9]. The structure and morphology of FeO is very important for predicting the properties of FeO NPs in terms of applications [10]. Hence, the

designing of NPs with different structures is significant. A lot of research has been dedicated to the synthesis of FeO NPs with different morphologies, structures, and forms such as nano-sheets, nano-rods, and nano-particles. However, these methods are expensive, energy-intensive, toxic, and need extreme conditions for operations. Therefore, biological methods for the synthesis of FeO NPs have been recognized to be fast, stable, environmentally viable, efficient, and cost-effective [11–14].

Synthesis of NPs in a biological way includes the use of plants and microorganisms such as bacteria, viruses, and fungi as reducing agents. However, due to the ease of handling plants, they have been receiving additional research attention. Green synthesis by use of plant-based sources involves the use of different parts of plants such as roots, stems, leaves, flowers, fruits, and seeds [14–16]. The NPs synthesized from plants are more stable in comparison to the NPs synthesized from microorganisms. Plants have several organic reducing agents that occur naturally which it simpler to produce NPs [17]. The relationship between plants and nanotechnology is referred to as green nanotechnology. There is a symbiotic relationship between plant science and nanotechnology as phytochemicals from plants are utilized for synthesizing NPs [18].

Coffee is ranked as the second product after petroleum that is being traded in the world. Coffee possesses various bioactive constituents such as phenols, flavonoids, steroids, alkaloids, saponins, and polysaccharides. These bioactive elements are termed phytochemicals of plants. Phytochemicals are present in coffee seeds (CSs) and they can be extracted and used as reducing agents as well as capping agents for the synthesis of FeO NPs. They play a critical role in converting the ions of iron to atoms of iron by depicting the building blocks of FeO NPs. Some of the most common micro-organisms that are pathogenic to humans are *Escherichia coli* (*E. coli*), *Staphylococcus aureus* (*S. aureus*), and *Aspergillus niger* (*A. niger*). A few strains of *S. aureus* are capable of resisting antibiotics like penicillin, vancomycin, methicillin, erythromycin, and tetracycline [19]. In this view, the NPs of FeO have shown anti-microbial potential in combating pathogens. Also, FeO NPs were reported to have good activity against several pathogenic micro-organisms such as fungi and bacteria due to their ability to produce reactive oxygen species [20].

In this study, we have reported the synthesis of FeO NPs from the aqueous extract of CSs for the first time and tested their efficiency in inhibiting the growth of microorganisms such as *E. coli, S. aureus,* and fungi *A. niger*. The particles were characterized to analyse the structures, morphology, and various other properties to understand their applications in diverse sectors. The biological activity of FeO NPs such as anti-oxidant, anti-microbial, and anti-fungal activities were carried out.

2 Materials and methods

2.1 Materials

High purity ferrous sulphate heptahydrate ($FeSO_4{\cdot}7H_2O$) was obtained from Rankem private limited, Mumbai, India, while CSs were obtained from standard dealers. Nutrient agar medium (NAM), potato dextrose agar (PDA), and acarbose were procured from Himedia. Triple distilled water was used throughout the reaction.

2.2 Preparation of CS extract

The commercially available coffee powder (10 g) was added to 100 mL of distilled water and boiled for 15 min at 70°C. Then, the extract was filtered by Whatman filter paper No. 42 and stored at 4–5°C for further investigation. Further, filter extract was used in the synthesis of FeO NPs.

2.3 Preparation of green FeO NPs

Green synthesis of FeO NPs was carried out with the coffee extract (100 mL) by heating to 40–60°C with continuous stirring using a magnetic stirrer. When the temperature of the extract reached 50°C, 150 mM of $FeSO_4{\cdot}7H_2O$ and 1 M NaOH solution were added and left for about 2 h till a brownish-black precipitate appeared [21]. Now this solution was cooled at room temperature and centrifuged at 4,000 rpm for 10 min with the help of centrifuge tubes. After centrifugation, it was washed three times with distilled water and once with ethanol. After washing, the pellets were dried at 100°C. Afterward, the collected particles were transferred to a ceramic crucible cup and heated in a furnace at 500°C for 2 h, and ground into powder with a mortar and pestle. The resultant brown powder is stored in an airtight container for characterization.

2.4 Microorganisms and culture conditions

Microbial cultures were prepared on potato dextrose agar plates and stored at 4°C, while the stock was grown in the

dark at 25°C in PDA for 7 days. A growth medium was prepared for use by mixing 80 g of glucose and fresh potato (500 mL) in 3.5 L of distilled water. Fresh potatoes were prepared by dicing 1 kg of potatoes and boiling them in 2 L of distilled water for 30 min. The medium was thus dispensed into 80 beakers with a capacity of 350 mL (50 mL per cup) and autoclaved at 121°C for 30 min. Inoculate vials with fresh microbial samples grown in PDA medium in Petri dishes for 7 days at 28°C. After 10 days of incubation under normal conditions (25°C), the culture media is filtered through filter paper to separate the filtrate and mycelium. The vaccine was shaken with ethyl acetate at 250 rpm for 20 min at room temperature. The extract is filtered and concentrated under vacuum at 40°C with a field evaporator to give a brown product (2 g).

2.5 Preparation of antibacterial assay

The method used to analyse antibacterial activity is a Well diffusion test on NAM [22]. This medium is poured aseptically into a Petri dish and left for 1 h to solidify. After that, fresh overnight cultures of *E. coli* and *S. aureus* (100 μg·mL^{-1}) were exposed to nutrient-rich agar using a vacuum and left in the plate for 15–20 min to absorb all bacteria. The wells were prepared by gel puncture (7–8 mm) under sterile conditions. The FeO NPs sample was placed in the well at different concentrations: 50, 100, and 150 μg·mL^{-1}. Plates were placed at room temperature for 30 min to allow the extract to disperse, then incubated at 37°C for 24 h to allow microbial growth. Antibody-containing materials inhibit the growth of bacteria after incubation by revealing a clear zone of inhibition (ZOI) around the well.

2.6 DPPH radical-scavenging activity

The radical scavenging activity of FeO NPs was measured according to their hydrogen donating ability or radical scavenging ability using stable radical DPPH. A solution of DPPH in ethanol (0.1 mM) was prepared and 1.0 mL of this solution was added to 2.0 mL of FeO NP at different concentrations (20–100 μg·mL^{-1}). Thirty minutes later, absorbance was measured at 517 nm. Ascorbic acid was used as a positive control. The low absorbance of the reaction mixture indicates greater free radical scavenging activity [23,24]. Free radical scavenging activity is expressed as the percentage inhibition of free radicals by the sample and the formula for the same is

$$D = \frac{A_{\text{ini}} - A_{\text{obs}}}{A_{\text{ini}}} \times 100$$

where A_{ini} refers to the absorbance of the reference/control sample (without FeO NPs). A_{obs} is the absorbance after the addition of FeO NPs

2.7 Alpha-amylase inhibition test

Inhibition testing was done using the DNSA method [25]. The solution contains α-amylase solution (1 U·mL^{-1}) at a concentration of 20 μg·mL^{-1} and 500 μL of 0.02 M sodium phosphate buffer (containing 6 mM NaCl, pH 6.9) with FeO NPs. The first incubation of the mixture was done at 37°C for 20 min.

After incubation, add 250 μL of 1% starch solution to the above buffer and incubate at 37°C for 15 min. Add 1 mL of dinitrosalicylic acid reagent to quench the reaction and then incubate in a boiling water bath for 10 min. Cool the tube and measure the absorbance at 540 nm. The reference sample contains all other reagents and enzymes except the test sample. Alpha-amylase inhibitory activity is expressed as percentage of inhibition.

Alpha-amylase inhibitory activity was calculated according to the following equation:

$$\%\text{Inhibition} = \frac{A_{i540} - A_{e540}}{A_{i540}} \times 100$$

where A_{i540} is the absorbance without FeO NPs. A_{e540} is the absorbance with FeO NPs.

2.8 Alpha-glucosidase inhibitory activity

Alpha-glucosidase inhibition was determined according to the standard method [26]. The analytical mix contains 150 mL of 0.1 M sodium phosphate buffer (containing 6 mM NaCl, pH 6.9) at a concentration of 20–410 mg mPL, 0.1 unit of α-glucosidase, and FeO NPs. Pre-incubate the mix at 37°C for 10 min. After incubation, add 50 μL of 2 mM *p*-nitrophenyl-α-D-glucopyranoside to 0.1 M sodium phosphate buffer and incubate at 37°C for 20 min. Stop the reaction by adding 50 μL of 0.1 M sodium carbonate (Na_2CO_3). Measure the absorbance at 405 nm. Tubes containing α-glucosidase but no FeO NPs were controlled with 100% enzyme activity and acarbose positive control.

$$\%\text{Inhibition} = \frac{A_{i405} - A_{e405}}{A_{i405}} \times 100$$

where A_{i405} is absorbance without FeO NPs. A_{e405} is absorbance with FeO NPs

2.9 Instrumentation

UV-Vis absorption spectra were obtained by Shimadzu 1900i at a wavelength of 200–800 nm. X-ray diffraction (XRD) spectra were recorded on a Bruker AXS D8 Advanced using Cuα radiation and Si(Li) position sensitive detector with a wavelength of 5,406 Å was used. Anton Paar TTK 450 accessory was added at 170°C–450°C. Features were obtained using scanning electron microscopy (SEM) JEOL Model JSM-6390LV. Resolution: 0.23 nm, lattice: 0.14 nm, 14 nm, 2,000× 1,500,000× magnification. Size and shape of the NPs were investigated using transmission electron microscopy (TEM) JEM 2100 plus, JEOL, Japan equipment.

3 Results and discussion

3.1 UV analysis

UV-Vis analysis was performed to confirm FeO synthesis by absorption spectroscopy and understand the optical nature. The UV-Vis absorption spectrum of FeO NPs is depicted in Figure 1 and the absorption spectra shows an absorption band at 293 nm which corresponds to the biomolecules. The strong and intense band at 293 nm represents the abundance of the biomolecules on the surface of the FeO NPs. The band at 293 nm is noticed to be broad and the broadening of the peak is just due to the presence of FeO NPs which extends beyond 500 nm [27].

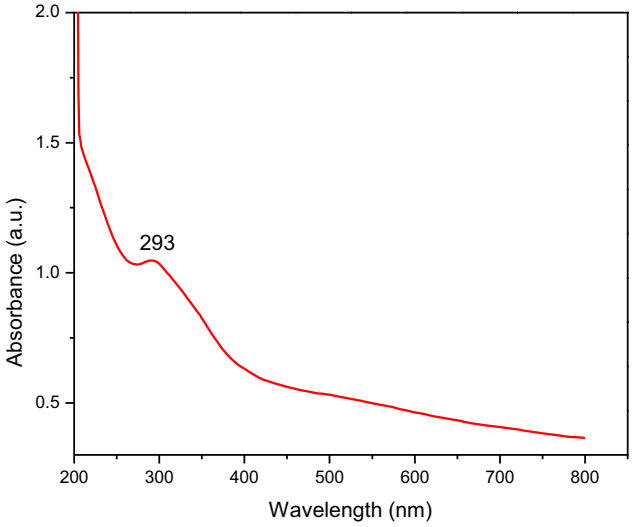

Figure 1: UV-Visible absorption spectra of as synthesized FeO NPs.

3.2 Structure and composition of FeO NPs

The XRD pattern of FeO NPs synthesized with coffee extract is presented in Figure 2. The examination revealed diffraction peaks at 32°, 35°, 38°, 55°, and 65°, these peaks indicated the formation of FeO NPs and is in good agreement with the literature (JCPDS 86-2316) [28]. The sharp and intense peaks revealed the NPs which were obtained from CSs having crystalline nature and Face centred cubic structure [29]. The XRD pattern confirms the formation of FeO NPs. FeO possesses a nonstoichiometric Fe*x*O configuration with an *x* value ranging from 0.83 to 0.96, alongside ordered Fe vacancies. This arrangement exhibits low chemical stability and may degrade into α-Fe. But in this study, the synthesized FeO is found to be stable and not prone to oxidation as suggested in the literature and our observations are in agreement with other similar works [30]. Debye–Scherrer formula is one of the most widely used formulas to estimate the crystallite size of NPs [31,32]. In this study, the Debye–Scherrer formula was used to estimate the average size of crystals and the average size of crystals were seen to be 36 nm. The interlayer spacing (*d*) is found to be 0.2732 nm and dislocation density (*δ*) is calculated to be 0.02739×10^{-14} lines·m^{-2}. The strain (ε) is found to be 4.26×10^{-3} and the peak broadening is due to the addition of the lattice strain [33].

3.3 Morphology

The NPs extracted from CSs were analysed by SEM to study the morphology of NPs. The results of SEM and EDAX analysis are presented in Figure 3(a–c). It can be observed that

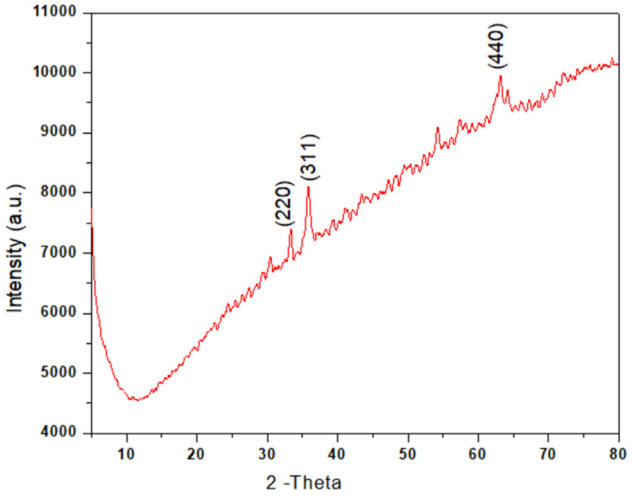

Figure 2: XRD analysis of FeO NPs synthesized from aqueous extract of CSs.

the NPs synthesized had agglomerates and were non-uniform in nature and appearance. The sizes of the particles were 20–50 nm approximately. The agglomerates were due to the buildup building blocks due to activities of reducing and capping agents of the coffee extract due to the magnetic activity [34–36].

The analysis of the elemental configuration was carried out by EDAX analysis. The results are presented in Figure 3b. It can be clearly seen that the peaks of Fe were observed at 6–7 keV, also the peaks at 0.5 and 0.7 keV showed the presence of C and O, respectively. These results were similar to the work reported by Sadasivam et al. [37]. The existence of carbon is due to the carbon available in the plant extract. The elemental analysis of the FeO NP is seen in Figure 3c. The distribution of Fe, C, and O and their amounts in percentage can be seen in Figure 3c.

The TEM analysis of FeO NPs was performed and the images are presented in Figure 4. It is noticed that the FeO NPs are at the nanoscale level and found to be less than 50 nm in scale as observed from the SEM and XRD analysis. The shapes of the NPs are observed to be non-spherical with irregularities and this might be due to the presence of various biomolecules acting as capping agents. However, the NPs are found to be agglomerated as seen in Figure 4 and this might be due to the interaction of biomolecules of coffee extract acting as building blocks of the FeO NPs.

3.4 HPLC analysis of CSs

Reverse phase HPLC was performed for the coffee extract to understand the number of biomolecules present in the

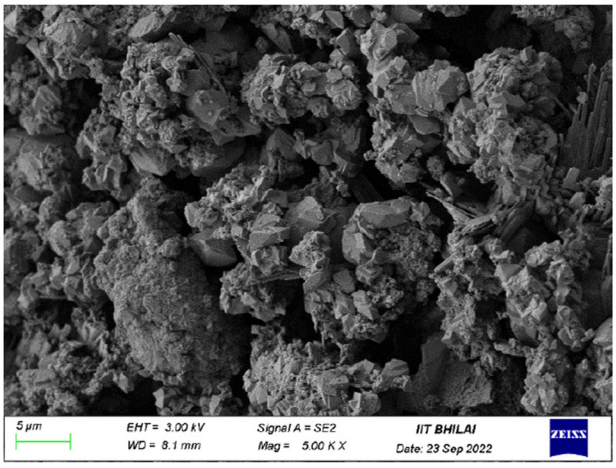

(a)

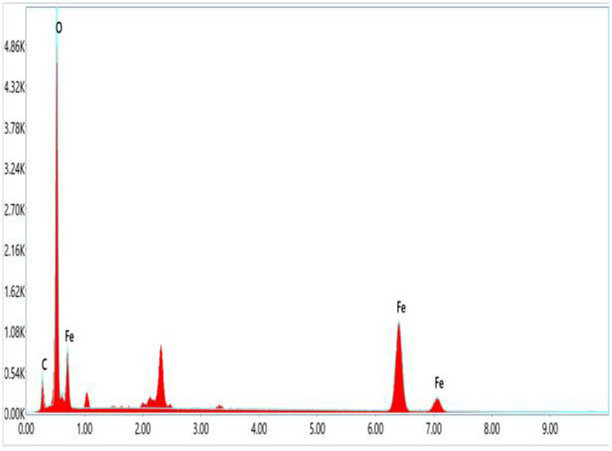

(b)

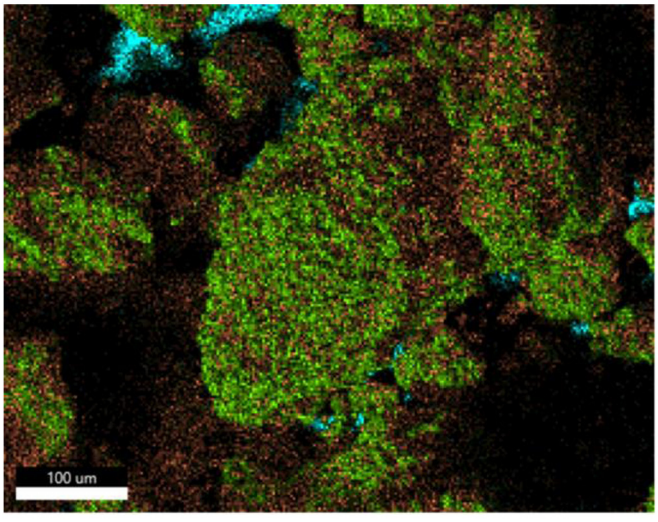

(c)

Element	Weight %	Atomic %	Net Int.	Error %
C K	13.5	27.0	36.4	11.4
O K	33.6	50.4	536.5	8.4
Fe K	52.9	22.7	354.4	2.8

Figure 3: (a) SEM micrographs, (b) EDAX analysis, and (c) elemental analysis of FeO NPs prepared from CSs aqueous extract.

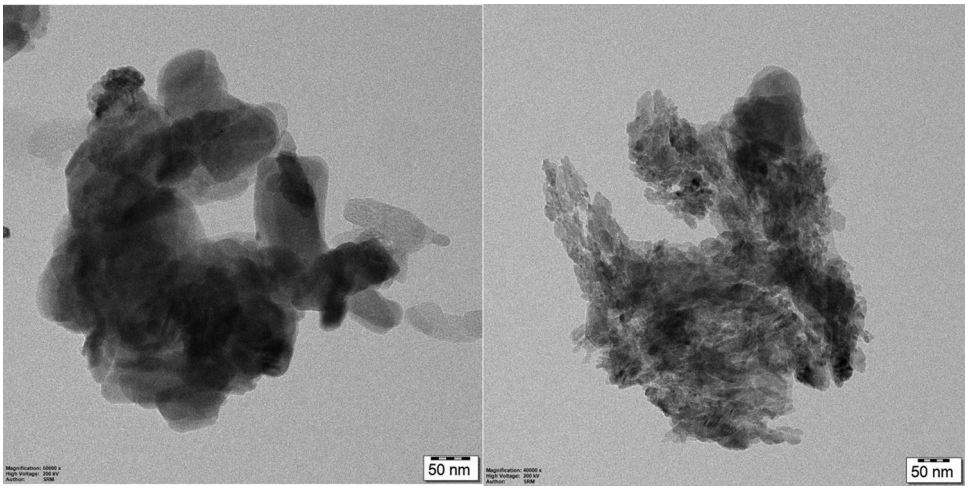

Figure 4: TEM images of FeO NPs prepared with coffee aqueous extract.

extract which can help in determining the molecules responsible for reduction and capping of the FeO NPs. The HPLC chromatogram is presented in Figure 5 and it can be seen that there are six peaks and two peaks are major suggesting that these two molecules are present majorly in the extract. Each peak at different retention times represents a type of molecule. These observations conclude that the coffee extract contains various biomolecules and these biomolecules can cap and stabilize the FeO NPs formations.

3.5 Antimicrobial activity of FeO NPs

The antibacterial activity of the FeO NPs synthesized using aqueous extract of coffee seeds was evaluated against bacteria *E. coli*, and *S. aureus* and it was observed that FeO NPs exhibited a good antimicrobial activity compared to the coffee aqueous extract. The antimicrobial activity is due to the interaction of the NPs onto the cell wall of the bacterial strains. However, the ZOI of standard Streptomycin and Vancomycin were found to be high compared to the FeO NPs suggesting that the FeO NPs are moderate and good microbial agents.

3.6 Antifungal activity of FeO NPs

The antifungal activities of the FeO NPs synthesized by green synthesis with different concentrations against fungus *A. niger* are presented in Figure 6. It can be clearly seen from

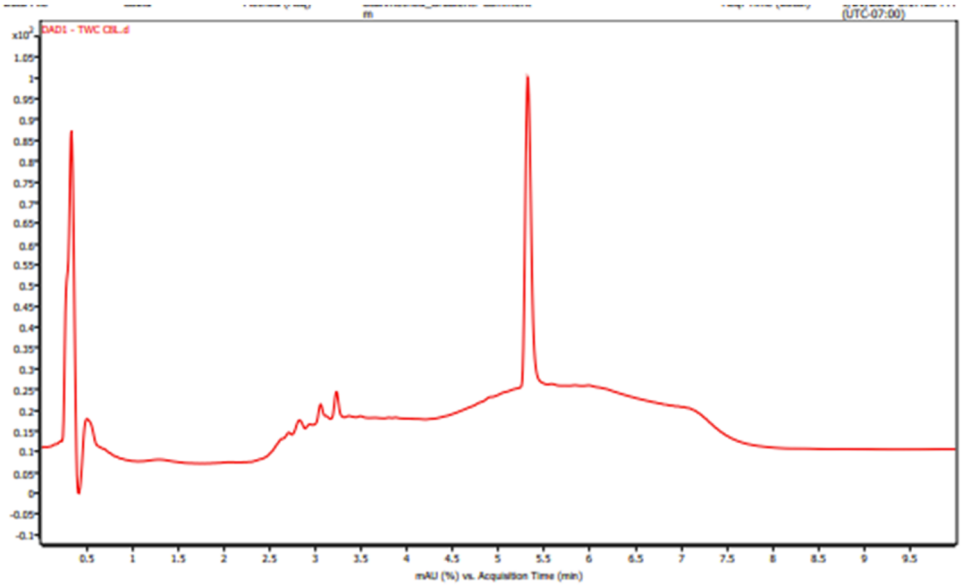

Figure 5: HPLC chromatogram of aqueous extract of CSs (C18 column, mobile phase: 70% ACN and 30% H_2O).

Figure 6: Antifungal activity of *A. niger* in the presence of FeO NPs prepared from CS extract.

Figure 6 that the FeO NPs displayed good antifungal activities against *A. niger* owing to its size and deposition on the fungus.

3.7 Antioxidant activity

Antioxidants have been recognized in their work against oxidative damage and have been associated with a reduced risk of chronic disease. Figure 7 shows the DPPH radical scavenging activity of FeO NPs at concentrations of 20–100 μg·mL^{-1} compared to standard (acarbose) and coffee bean extract. IC50 values of FeO NPs were higher compared to acarbose acid and coffee bean extract. The results showed that the free radical

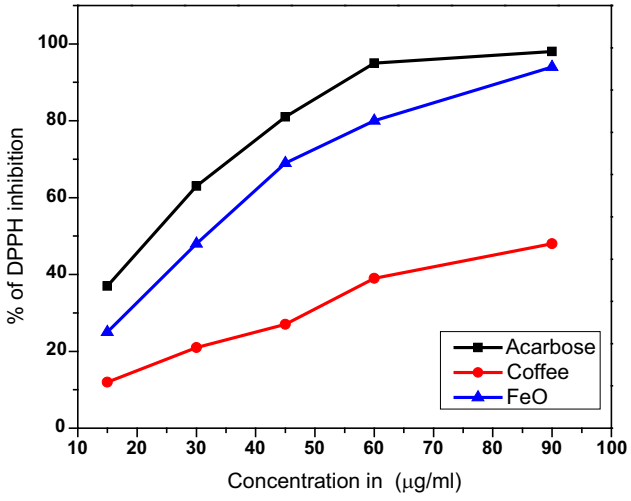

Figure 7: DPPH inhibition activity of acarbose, CS extract, and FeO NPs.

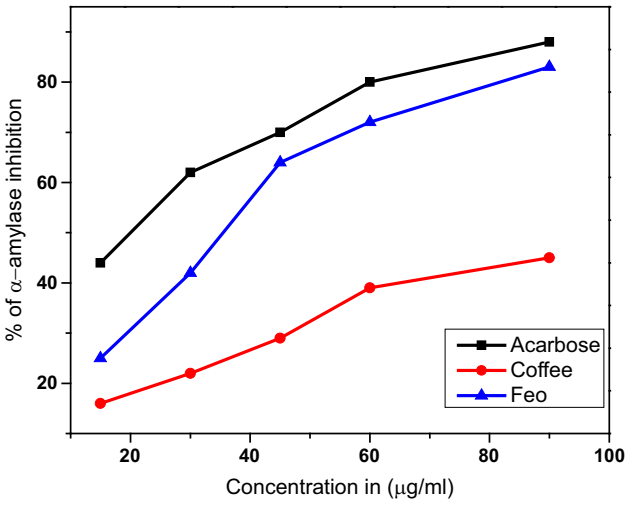

Figure 8: α-Amylase inhibition activity of acarbose, CS extract, and FeO NPs.

scavenging of FeO NPs slightly increased with the dosage. This result is consistent with the DPPH activity of FeO NPs reported in the literature [38–40].

3.8 Inhibition of α-amylase and α-glucosidase by FeO NPs

Carbohydrate-digesting enzymes such as pancreatic α-amylase and intestinal α-glucosidase are responsible for breaking down oligosaccharides and disaccharides into monosaccharides suitable for absorption. Inhibiting two digestive enzymes is particularly useful in the treatment of non-insulin diabetes, as it slows the release of sugar from the blood. As shown in Figures 8 and 9, the results

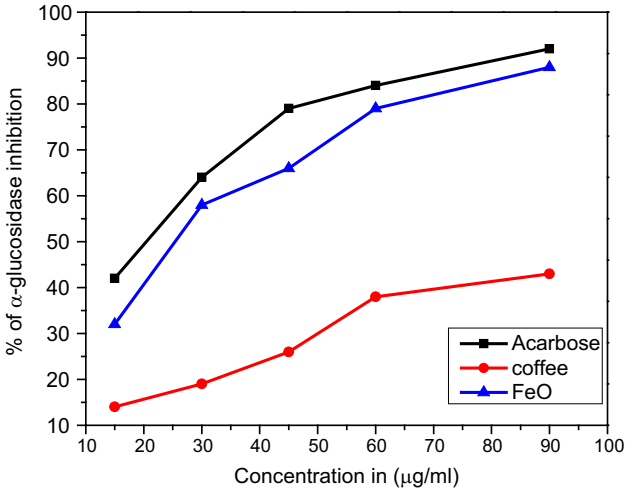

Figure 9: α-Glucosidase inhibition activity of acarbose, CS extract, and FeO NPs.

showed that α-amylase and α-glucosidase were significantly affected in a concentration-dependent manner after incubation with different FeO NP concentrations. As the concentration of FeO NPs increased, the level of enzyme activity decreased significantly. It can be seen from Figures 8 and 9 that the IC 50 values for amylase and α-glucosidase of FeO NPs were similar to those obtained in previous reports.

According to many *in vivo* studies, inhibition of α-amylase and α-glucosidase is considered one of the most effective treatments for diabetes.

4 Conclusion

As NPs exhibit many attractive properties and functions in many applications, the study of NP synthesis method has recently become a major area of interest in science and engineering. Biosynthesis of FeO NPs using green sources is an effective method due to its simplicity, environmental protection, and cost. In this study, FeO NPs were successfully produced by bioreducing ferric chloride solution using CS aqueous extract. This is evidenced by UV-Vis spectroscopic analysis, which shows a broad absorption peak at 293 nm. The XRD, SEM, and TEM investigations propounds that the size of the FeO NPs are between 20 and 50 nm in range with non-spherical shape. The synthesized FeO NPs also exhibited potent antibacterial activity against pathogenic bacteria whose MICs inhibited the growth of *Escherichia coli* and *Staphylococcus aureus*. The antioxidant activity of the synthesized FeO was analysed and it was seen that the FeO NPs had excellent inhibiting activity against DPPH, α-amylase, and α-glucosidase in comparison with acarbose and coffee extract. The results conclude that the FeO NPs synthesized via green synthesis using aqueous extract of CSs found to have versatile biological significance and further investigations is required to incorporate the FeO NPs in the pharmaceutical formulations.

Acknowledgements: The authors extend their appreciation to the Researchers Supporting Project number (RSPD2024R739) at King Saud University, Riyadh, Saudi Arabia.

Funding information: This research was funded by King Saud University, Riyadh, Saudi Arabia (RSPD2024R739).

Author contributions: Abdulaziz Alangari: formal analysis and visualization; Mohammed S Alqahtani: formal analysis, methodology, and resources; Mudassar Shahid: project administration and original draft writing; Rabbani Syed: writing and reviewing and validation; Mukesh Goel: visualization and editing; R. Lakshmipathy: writing – reviewing and editing; Kirtanjot Kaur: formal analysis.

Conflict of interest: Authors state no conflict of interest.

Data availability statement: The datasets generated during and/or analysed during the current study are available from the corresponding author on reasonable request.

References

[1] Moradnia F, Fardood ST, Ramazani A, Osali S, Abdolmaleki I. Green sol–gel synthesis of $CoMnCrO_4$ spinel nanoparticles and their photocatalytic application. Micro Nano Lett. 2020;15(10):674–7. doi: 10.1049/mnl.2020.0189.

[2] Elakkiya GT, Balaji GL, Padhy H, Lakshmipathy R. Synthesis of silver nanoplates using regenerated watermelon rind and their application. Mater Today:-Proc. 2022;55(2):240–5. doi: 10.1016/j.matpr.2021.06.370.

[3] Saeid TF, Farzaneh M, Reza F, Rouzbeh A, Salman J, Ali R, Mika S. Facile green synthesis, characterization and visible light photocatalytic activity of $MgFe_2O_4$@$CoCr_2O_4$ magnetic nanocomposite. J Photoch Photobio A. 2022;423:113621. doi: 10.1016/j.jphotochem.2021.11362.

[4] Taghavi FS, Ramazani A, Asiabi PA. A novel green synthesis of copper oxide nanoparticles using a henna extract powder. J Struct Chem. 2018;59:1737–43. doi: 10.1134/S0022476618070302.

[5] Andal V, Buvaneswari G, Lakshmipathy R. Synthesis of $CuAl_2O_4$ nanoparticle and its conversion to CuO nanorods. J Nanomater. 2021;2021:8082522. doi: 10.1155/2021/8082522.

[6] Vasantharaj S, Selvam S, Mythili S, Palanisamy S, Kavitha G, Muthiah S, et al. Synthesis of ecofriendly copper oxide nanoparticles for fabrication over textile fabrics: Characterization of antibacterial activity and dye degradation potential. J Photochem Photobiol B. 2019;191:143–9. doi: 10.1016/j.jphotobiol.2018.12.026.

[7] Mohsen B, Nezamzadeh-Ejhieh A. Effect of supporting and hybridizing of FeO and ZnO semiconductors onto an Iranian clinoptilolite nano-particles and the effect of ZnO/FeO ratio in the solar photodegradation of fish ponds waste water. Mat Sci Semicon Proc. 2014;27:833–40. doi: 10.1016/j.mssp.2014.08.030.

[8] Zarifeh-Alsadat M, Nezamzadeh-Ejhieh A. Removal of phenol content of an industrial wastewater via a heterogeneous photodegradation process using supported FeO onto nanoparticles of Iranian clinoptilolite. Des Water Treat. 2016;57:16483–94. doi: 10.1080/19443994.2015.1087881.

[9] Moradnia F, Fardood ST, Ramazani A. Green synthesis and characterization of $NiFe_2O_4$@$ZnMn_2O_4$ magnetic nanocomposites: An efficient and reusable spinel nanocatalyst for the synthesis of tetrahydropyrimidine and polyhydroquinoline derivatives under microwave irradiation. Appl Organomet Chem. 2024;38(3):e7315. doi: 10.1002/aoc.7315.

[10] Abbas N, Nezamzadeh-Ejhieh A. Preparation, characterization, and investigation of the catalytic property of α-Fe_2O_3-ZnO nanoparticles in the photodegradation and mineralization of methylene blue. Chem Phy Lett. 2020;752:137587. doi: 10.1016/j.cplett.2020.137587.

[11] Vasantharaj S, Sathiyavimal S, Senthilkumar P, Lewis Oscar F, Pugazhendhi A. Biosynthesis of iron oxide nanoparticles using leaf

extract of Ruellia tuberosa: Antimicrobial properties and their applications in photocatalytic degradation. J Photochem Photobiol B Biol. 2019;192:74–82. doi: 10.1016/j.jphotobiol.2018.12.025.
[12] Sathiyavimal S, Seerangaraj V, Veerasamy V, Mythili S, Govindaraju R, Thamaraiselvi K, et al. Green chemistry route of biosynthesized copper oxide nanoparticles using Psidium guajava leaf extract and their antibacterial activity and effective removal of industrial dyes. J Environ Chem Eng. 2021;9:105033. doi: 10.1016/j.jece.2021.105033.
[13] Saif S, Tahir A, Chen Y. Green synthesis of iron nanoparticles and their environmental applications and implications. Nanomater. 2016;6:209. doi: 10.3390/nano6110209.
[14] Kalaiarasi R, Jayallakshmi N, Venkatachalam P. Phytosynthesis of nanoparticles and its applications. plant cell biotechnol. Mol Biol. 2010;11:1–16. doi: 10.5555/20133284851.
[15] Shukla R, Chanda N, Katti KK, Katti KV. Green nanotechnology – A sustainable approach in the nanorevolution. In Sustainable preparation of metal nanoparticles: Methods and application. RSC Publishing; 2012. p. 144–56.
[16] Vayalil PK. Date fruits (Phoenix dactylifera Linn): An emerging medicinal food. Crit Rev Food Sci Nutr. 2012;52:249–71. doi: 10.1080/10408398.2010.499824.
[17] Taleb H, Maddocks SE, Morris RK, Kanekanian AD. Chemical characterisation and the anti-infammatory, anti-angiogenic and antibacterial properties of date fruit (Phoenix dactylifera L.). J Ethnopharmacol. 2016;194:457–68. doi: 10.1016/j.jep.2016.10.032.
[18] Al Harthi S, Mavazhe A, Al Mahroqi H, Khan SA. Quantifcation of phenolic compounds, evaluation of physicochemical properties and antioxidant activity of four date (Phoenix dactylifera L.) varieties of Oman. J Taibah Univ Med Sci. 2015;10:346–52. doi: 10.1016/j.jtumed.2014.12.006.
[19] Yasin BR, El-Fawal HA, Mousa SA. Date (Phoenix dactylifera) polyphenolics and other bioactive compounds: A traditional islamic remedy's potential in prevention of cell damage, cancer therapeutics and beyond. Int J Mol Sci. 2015;16:30075–90. doi: 10.3390/ijms161226210.
[20] Al-Daihan S, Bhat RS. Antibacterial activities of extracts of leaf, fruit, seed and bark of Phoenix dactylifera. Afr J Biotechnol. 2012;11:10021–5. doi: 10.5897/AJB11.4309.
[21] Lakshminarayanan S, Shereen MF, Niraimathi KL, Brindha P, Arumugam A. One-pot green synthesis of iron oxide nanoparticles from Bauhinia tomentosa: Characterization and application towards synthesis of 1, 3 diolein. Sci Rep. 2021;11:8643. doi: 10.1038/s41598-021-87960-y.
[22] Shamaila S, Zafar N, Riaz S, Sharif R, Nazir J, Naseem S. Gold nanoparticles: an efficient antimicrobial agent against enteric bacterial human pathogen. Nanomaterials. 2016;6(4):71. doi: 10.3390/nano6040071.
[23] Pankhurst QA, Connolly J, Jones S, Dobson J. Applications of magnetic nanoparticles in biomedicine. J Phys D Appl Phys. 2003;36:R167. doi: 10.1088/0022-3727/36/13/201.
[24] Kavitha K, Baker S, Rakshith D, Kavith H, Harini BP, Satish S. Plants as green source towards synthesis of nanoparticles. Int Res J Biol Sci. 2013;2:66–76.
[25] Jain, A, Jain, R, Jain, S. Quantitative analysis of reducing sugars by 3, 5-dinitrosalicylic acid (DNSA Method). Basic Techniques in biochemistry, microbiology and molecular biology. Springer Protocols Handbooks. New York, NY: Humana; 2020.
[26] Dej-adisai S, Rais IR, Wattanapiromsakul C, Pitakbut T. Alpha-glucosidase inhibitory assay-screened isolation and molecular docking model from Bauhinia pulla active compounds. Molecules. 2021;26:5970. doi: 10.3390/molecules26195970.
[27] Karpagavinayagam P, Vedhi C. Green synthesis of iron oxide nanoparticles using Avicennia marina flower extract. Vacuum. 2019;160:286–92. doi: 10.1016/j.vacuum.2018.11.043.
[28] Narges A, Nezamzadeh-Ejhieh A. Modification of clinoptilolite nanoparticles with iron oxide: Increased composite catalytic activity for photodegradation of cotrimaxazole in aqueous suspension. Mat Sci Semicon Proc. 2015;31:684–92. doi: 10.1016/j.mssp.2014.12.067.
[29] Nezamzadeh-Ejhieh A, Shirzadi A. Enhancement of the photocatalytic activity of ferrous oxide by doping onto the nano-clinoptilolite particles towards photodegradation of tetracycline. Chemosphere. 2014;107:136–44. doi: 10.1016/j.chemosphere.2014.02.015.
[30] Shirin G, Nezamzadeh-Ejhieh A. A double-Z-scheme ZnO/AgI/WO_3 photocatalyst with high visible light activity: Experimental design and mechanism pathway in the degradation of methylene blue. J Mol Liquid. 2021;322:114563. doi: 10.1016/j.molliq.2020.114563.
[31] Fardood TS, Moradnia F, Moradi S, Forootan R, Yekke Zare F, Heidari M. Eco-friendly synthesis and characterization of α-Fe_2O_3 nanoparticles and study of their photocatalytic activity for degradation of Congo red dye. Nanochem Res. 2019;4(2):140–7. doi: 10.22036/NCR.2019.02.005.
[32] Farzaneh M, Fardood TS, Ali R, Gupta VK. Green synthesis of recyclable $MgFeCrO_4$ spinel nanoparticles for rapid photodegradation of direct black 122 dye. J Photochem Photobiol A. 2020;392:112433. doi: 10.1016/j.jphotochem.2020.112433.
[33] Salesi S, Nezamzadeh-Ejhieh A. Boosted photocatalytic effect of binary AgI/Ag_2WO_4 nanocatalyst: characterization and kinetics study towards ceftriaxone photodegradation. Environ Sci Pollut Res. 2022;29:90191–206. doi: 10.1007/s11356-022-22100-1.
[34] Mukunthan K, Balaji S. Silver nanoparticles shoot up from the root of Daucus carrota (L.). Int J Green Nanotechnol. 2012;4:54–61. doi: 10.1080/19430892.2012.654745.
[35] Herlekar M, Barve S, Kumar R. Plant-mediated green synthesis of iron nanoparticles. J Nanopart. 2014;2014:140614. doi: 10.1155/2014/140614.
[36] Fazlzadeh M, Rahmani K, Ahmad Z, Hossein A, Nasiri F, Khosravi R. A novel green synthesis of zero valent iron nanoparticles (NZVI) using three plant extracts and their efficient application for removal of Cr (VI) from aqueous solutions. Adv Powder Technol. 2017;28:122–30. doi: 10.1016/j.apt.2016.09.003.
[37] Sadhasivam S, Vinayagam V, Balasubramaniyan M. Recent advancement in biogenic synthesis of iron nanoparticles. J Mol Struct. 2020;1217:128372. doi: 10.1016/j.molstruc.2020.128372.
[38] Hoag GE, Collins JB, Holcomb JL, Hoag JR, Nadagouda MN, Varma RS. Degradation of bromothymol blue by 'greener' nanoscale zero-valent iron synthesized using tea polyphenols. J Mater Chem. 2009;19:8671–7. doi: 10.1039/B909148C.
[39] Kumar KM, Mandal BK, Kumar KS, Reddy PS, Sreedhar B. Biobased green method to synthesise palladium and iron nanoparticles using Terminalia chebula aqueous extract. Spectrochim Acta A Mol Biomol Spectrosc. 2013;102:128–33. doi: 10.1016/j.saa.2012.10.015.
[40] Makarov VV, Makarova SS, Love AJ, Olga VS, et al. Biosynthesis of stable iron oxide nanoparticles in aqueous extracts of Hordeum vulgare and Rumex acetosa plants. Langmuir. 2014;30:5982–8. doi: 10.1021/la5011924.